Robert D. Lawrence
James H. Herzog
Oregon State University
Corvallis, OR 97331

Geology and Forestry Classification from ERTS-1 Digital Data

The geology and forest cover of two areas in Central Oregon were classified based on computer classification of ERTS-1 digital data.

Introduction

The ERTS-1 Satellite was launched by NASA in July 1972 into a 500 mile sun-synchronous orbit. The satellite is equipped with two sensors which, for the first time, allow scientists and engineers to freely experiment with the potential of high quality digital data procured from a stable space platform. The primary data collection device on board the satellite is a multi-spectral scanner that records reflected ground radiation in four distinct spectral bands: green (0.5 - 0.6 μm), red (0.6 - 0.7 μm), infrared (0.7 - 0.8 μm), and near infrared (0.8 - 1.1 μm). The optics of the satellite scan across the surface of the earth in a direction perpendicular to the flight path. A vertical raster is provided by the forward motion of the satellite. Each frame of ERTS data covers 100 by 100 nautical miles. The ground resolution of each digital datum is approximately 1.16 acre. ERTS data can be used to reconstitute photograph-like imagery for each band or some combination of bands, to produce a spectral signature for each individual earth resolution element and to produce a classification map based on signature types. The photographic product has been widely discussed and used according to conventional and exotic photo-interpretation techniques. The latter two products are the result of some form of computer analysis of the digital data.

Abstract: *Computer classifications into seven and ten classes of two areas in central Oregon of interest to geology and forestry demonstrate the extraction of information from ERTS-1 data. The area around Newberry Caldera was classified into basalt, rhyolite obsidian, pumice flats, Newberry pumice, ponderosa pine, lodgepole pine and water classes. The area around Mt. Washington was classified into two basalts, three forest, two clearcut, burn, snow, and water classes. Both also include an unclassified category. Significant details that cannot be extracted from photographic reconstitutions of the data emerge from these classifications, such as moraine locations and paleo-wind directions. Spectral signatures for the various rocks are comparable to those published elsewhere.*

Rowan (1972) has published spectral signatures for some common rocks and minerals. He finds that spectral response in the near-IR depends largely on the iron content of the material. Vincent (1973) has applied this approach to ERTS data for iron deposits in Wyoming. Areas of recent volcanism in central Oregon (Figure 1) provide an opportunity to examine the spectral response of rocks of varied composition, texture, and iron content

Photogrammetric Engineering and Remote Sensing,
Vol. 41, No. 10, October 1975, pp. 1241-1251.

in this study. Rhyolite obsidian, rhyolite ash and basalt flows are present that are young enough (less than a few thousand years old) to produce rather pure signatures. These can be compared with the signatures of progressively older rocks that are increasingly altered and vegetated.

Computer classifications of ERTS data have been produced by a number of workers, mostly utilizing user supplied training sets. Successful classifications have differentiated types of agricultural croplands (Bauer and Cipra, 1973, Baumgardner and Dillman, 1973), and broad natural area categories (Kirvida and Johnson, 1973; and Thomson and Roller, 1973). All of these efforts and others of a similar nature have concentrated on the extraction of land-use and vegetational information. Similar classifications of two volcanic areas of central Oregon, described below, were performed with training sets selected by a geologist. These classifications display both gross and detailed geologic information content, and considerable forest information as well. A similar effort in an area of sedimentary rocks is reported by Melhorn and Sinnock (1973).

Study Areas

The two study areas selected for the present effort are in central Oregon (Figure 1) where young volcanic rocks are exposed at the surface. The Newberry area covers the crest of Newberry Volcano, a young caldera developed around the central vent of a large basaltic shield volcano (Higgins, 1973). Very recent rhyolitic obsidian flows, less than 1720±250 years old, are present on the floor of the caldera (Higgins, 1969) and recent basalt flows (radiometric age unknown) are present on the flanks of the volcano. Older rhyolite domes and ash and basaltic cinder cones are also abundant. Much of the area is blanketed by Newberry (1720 years old) and Mazama (6500 years old) pumaceous ash. The Mt. Washington area centers on Belknap Crater and Mt. Washington. Basalt flows of various young ages (1500 to 4000 years) erupted from Belknap Crater, North Sister, and other vents in the area (Taylor, 1968, and personal communication, 1974). Both areas have extensive forest covers where the very young rocks are not exposed. The greatest variety of forestry interest is in the Mt. Washington area. Details on the geology used in the following discussion of these two areas rely heavily on the work of Higgins (1969, 1973) and Taylor (1968).

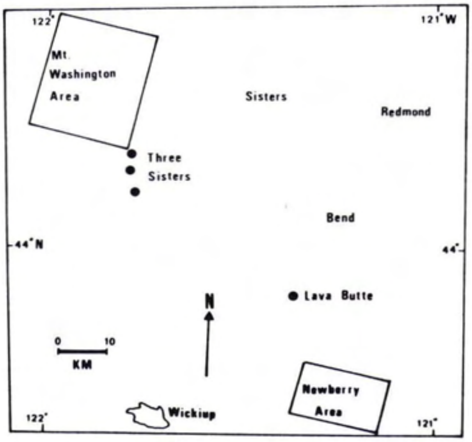

Fig. 1. Central Oregon study areas.

Classification

Classification is the process in which a set of rules is used to assign each ground resolution element to one of several classes by machine or human methods. In the case of a human photo-interpreter, classification extends results obtained in local, known regions, to surrounding, unknown regions. Either classification method requires the use of selected characteristics. The photo-interpreter commonly uses color or tone, texture, and shape to identify similar regions. In computer classification of ERTS data, the magnitudes of the four pieces of spectral information are used as characteristics. It is assumed that two regions on the earth that are seasonally identical will have identical or very similar sets of numbers (spectral signatures). Regions which differ should have different signatures.

Computer classification eliminates the repetitious judgment of a human operator and increases the detail of the classification. Because of the magnitude of the data, a human operator could not possibly individually evaluate and classify the approximately 7.5 million ground resolution elements of an ERTS scene. However, extensive interaction with a human interpreter is still required as the "ground truth" requirements are very similar to those of photo-interpretation. Known examples of the classes selected for classification must be identified for the computer as training sets. The computer abstracts the mean and standard deviation of each of the four spectral measurements for all elements in each training set.

For each class $(1, 2, \ldots, i)$ the computer constructs a prototype vector,

$$F_i = \begin{bmatrix} f_{ia} \\ f_{ib} \\ f_{ic} \\ f_{id} \end{bmatrix}$$

where a, b, c, and d indicate the four spectral bands. Each element of this vector is the mean of the corresponding training set for that class. Classification of the unknown vector is performed based on the Euclidean distance between the unknown vector and each of the prototype vectors. Each unknown vector, F_x, is constructed from the four data of a given resolution element such that

$$F_x = \begin{bmatrix} f_a \\ f_b \\ f_c \\ f_d \end{bmatrix}$$

and a set of D_i are calculated aginst the prototype vectors as

$$D_i = (f_{ia} - f_a)^2 + (f_{ib} - f_b)^2 + (f_{ic} - f_c)^2 + (f_{id} - f_d)^2$$

The threshold value, T_i, for each class is defined by the human operator. This value is included in order to allow a "none of these" classification if the distance is larger than that expected for a given class. Now D is the minimum value of the set of D_i and if $D \leq T_i$, F_x is assigned to class i, but if $D > T_i$, F_x is assigned to "none of these". Tables 1 and 2 show the values of band means and thresholds for the prototype vectors used in the two classifications discussed herein.

Results

The computer classifications of the two areas are shown in Figure 2 and Plate 1 (portions of ERTS frames 1076-18213 and 1041-18265, respectively) with the symbol and color coding presented on Tables 1 and 2. Eight classes are used on the Newberry area classification and eleven classes on the Mt. Washington area classification. These classifications have been evaluated through the use of published geologic maps and RB-57 high flight imagery (NASA Flights 72-114 and 73-106). The brief class denotations listed on Tables 1 and 2 represent the character of the training sets used. In some cases the actual class is more varied. Figure 2 and Plate 1 are, therefore, evaluated in two different manners. First, they are treated as simple automatic classifications of the data, and classification accuracy is evaluated both subjectively and quantitatively. Second, they are treated from the perspective of a photo-interpreter, and information is extracted from variations that are treated as classification errors in the first approach. This second method allows information details to be extracted from the data that are either impossible or extremely difficult to see on the photographic ERTS imagery, and are also beyond the ability of the automatic classifier to decipher. Thus we find that the maximum information is extracted from ERTS data by a combination of machine and human interpretation. Figures 3 and 4 are interpretive overlays drawn from the automatic classifications showing some of the significant features that are present on them. Reference to these figures will clarify much of the discussion that follows. Areas used to evaluate the classifications quantitatively were determined by planimeter from maps and aerial photographs. Particularly for the smaller areas this method may involve as much or more error as the digital determination.

Newberry Lithologic Classes

Four classes based on lithology are used in the Newberry classification. These are bare basalt, bare rhyolite obsidian, pumice flat, and Newberry pumice. The first three are quite successful; the last proves to be a poor class. For the three good classes a comparison of the area classified to that measured is shown on Table 3. The two larger classes reflect results for the entire classification, while the smaller ones are for selected areas. The apparent precision of the results for the obsidian flows is the result of rather numerous, but mutually compensating, errors of commission and omission. However, the areas of the bare obsidian flows are all identified and blocked out, including even the very small one in the vent of the Central Pumice Cone (8 on Figure 3). The omission errors result in less than the total flow area being identified, while the commision errors are mostly single points scattered widely over the remainder of the classification. This is an excellent example of the role of the threshold value. Lowering the threshold will increase the relative number of omission errors, whereas raising the threshold will increase the relative number of commission errors. Either represents a departure from the overall precision of the statistical result. This level of statistical success is not possible with the basalt flow and pumice flat classes. In these cases most of the errors are of commission. For example, an edge effect occurs

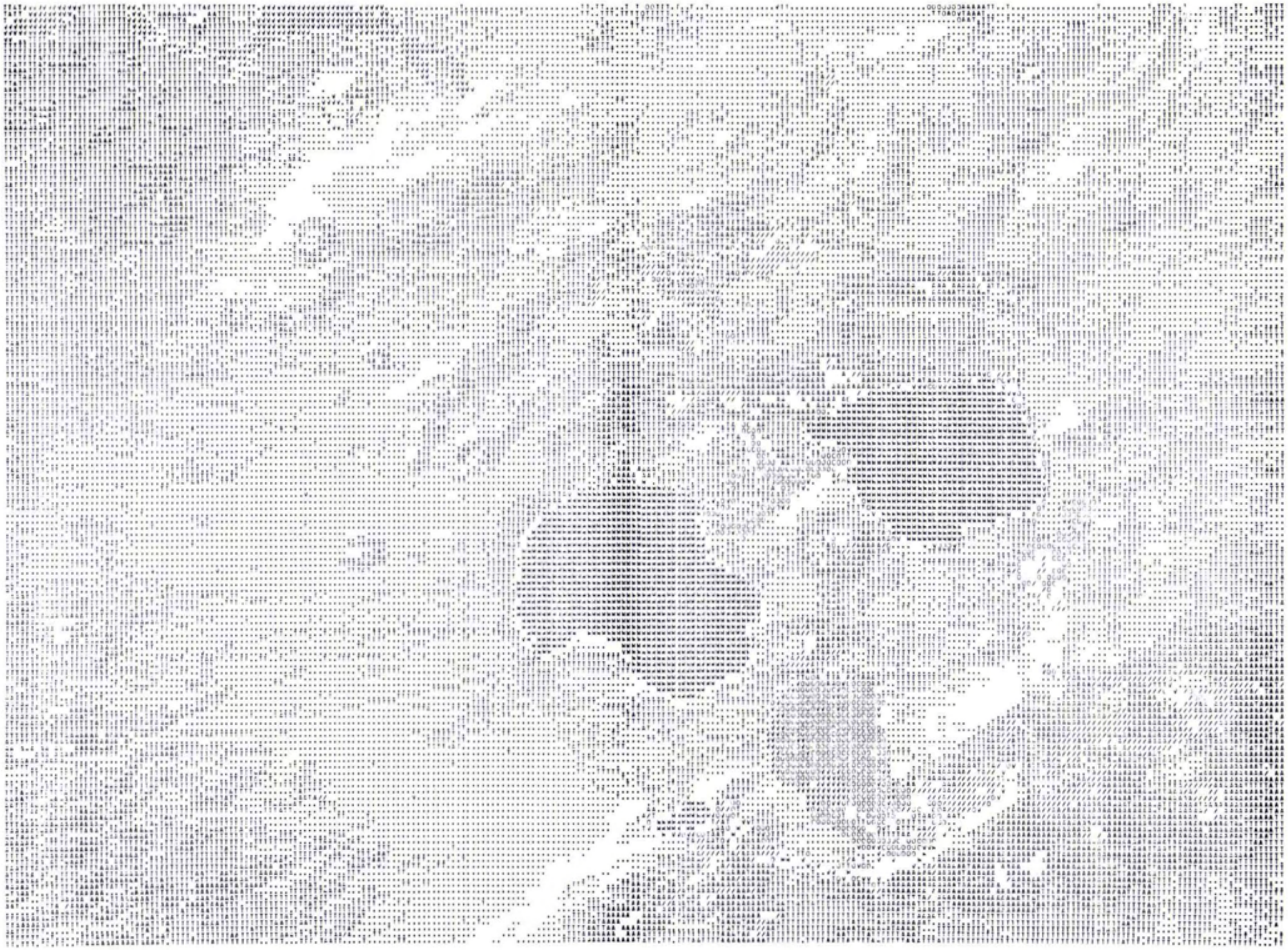

FIG. 2. Computer classification of the Newberry area of ERTS-1 frame 1076-18213, 7 October 1972 (see Table 1 for coding).

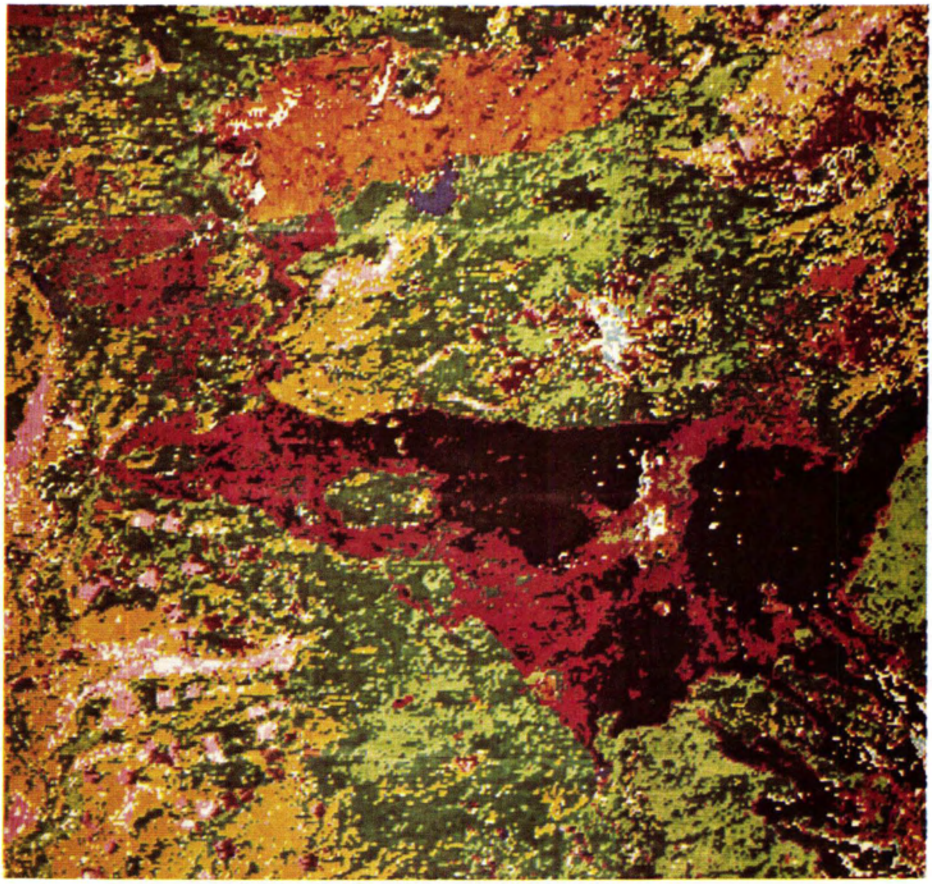

PLATE 1. Computer classification of the Mt. Washington area of ERTS-1 frame 1041-18265, 2 September 1972 (see Table 2 for coding).

TABLE 1. STATISTICS ON NEWBERRY CLASSIFICATION.

Class	symbol	Acres	%	Band Means 4	5	6	7	Threshold
Bare basalt flow	V	246	2	8.14	5.66	4.99	3.98	4.00
Bare rhyolite obsidian	D	885	2	10.94	9.01	7.43	5.71	15.00
Pumice flats	I	610	1	14.54	14.50	14.89	13.31	40.00
Newberry Pumice in SE (south slopes elsewhere)	A	5,287	12	9.29	7.50	11.41	12.65	14.00
Ponderosa Pine forest (open)	T	17,446	39	7.80	4.50	8.51	9.86	20.00
Lodgepole Pine forest (dense)	·	15,008	34	7.81	4.79	6.82	7.55	4.00
Water	W	2,282	5	6.93	2.13	1.11	1.00	5.00
Unclassified		2,007	5					
Total		44,246	100					

TABLE 2. STATISTICS ON MT. WASHINGTON CLASSIFICATION.

Class	Color Code	Acres	%	Band Means 4	5	6	7	Threshold
Younger Basalt	Black	16,551	12.4	8.89	6.23	5.55	4.54	10.00
Older Basalt	Red	14,417	10.8	8.84	6.41	8.77	9.19	12.00
Water	Dk. Blue	418	0.3	7.66	3.21	2.17	1.22	7.00
Forest 1—Mixed	Dk. Green	47,688	35.7	8.24	4.99	10.06	12.21	10.00
Forest 2—Douglas Fir or Ponderosa Pine	Yellow	17,283	12.9	8.12	4.63	13.19	16.50	6.00
Forest 3—Lodgepole Pine	Lt. Green	13,164	9.9	7.65	4.59	8.47	9.90	12.00
Clearcut 1—Little revegetation	Brown	5,982	4.5	10.87	9.94	14.43	16.74	18.00
Clearcut 2—Brushy revegetation	Pink	3,872	2.9	10.30	7.72	17.32	21.41	21.00
Snow	Lt. Blue	322	0.2	41.76	43.05	37.76	28.10	70.00
Burn	Orange	7,257	5.4	11.52	10.26	11.94	12.18	13.00
Unclassified	White	6,678	5.0					
Total		133,632	100.0					

along water such that a single resolution element which covers about half water and half land will be classified as basalt. Likewise, scattered forest on obsidian is classified as basalt. In each case, a subclass of significant size is present which has the same spectral signature as basalt. The small area of basalt within the classification, less than a square mile, makes these effects particularly significant. Thus, although the total area classified as basalt is 24% greater than the measured area of basalt flows, when only a single flow is measured it is significantly underclassified (compare the two basalt entires on Table 3). The results for the pumice flats are probably similar except that the classification is nearly correct for isolated areas. The degree of commission error is difficult to evaluate, however, because the very small areas of open pumice are not readily distinguished on the available photography. The class created on the thick deposits of Newberry pumice in the southeastern part of the classification is not highly successful as a unique lithologic class. This is largely because most of the classification is blanketed by pumice with varying densities of forest cover so that the intended class is not unique. Thus, most of the highly illuminated south slopes are included in the Newberry pumice class.

MT. WASHINGTON LITHOLOGIC CLASSES

Almost the entire area is underlain by basaltic flow materials in various stages of weathering. Two very successful basalt classes were developed which separate the most recent flows. The younger basalt lava flows are mostly bare rock with lichen and scattered blackberry, manzanita, and other bushes. The older basalt lava flows have scattered trees in addition to the vegetation just mentioned. This corresponds very closely with the separation of flows that are less than 3000 years old by radiocarbon dates and flows that are greater than 3000 years old (Taylor, 1968). The primary error in the age distinction is that one of the younger flows from Belknap extends west across highway 126, but the more moist climate on this western slope has resulted in sufficient weathering and revegetation to change the classification. Much the same effect occurs on the older flows, resulting in their being classed as forest. The kind of commission errors discussed under the Newberry lithologic units

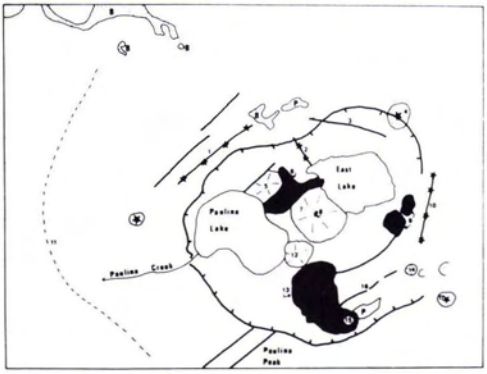

FIG. 3. Interpretation of classification of the Newberry area.

Number Symbols

1 Red Slide Conder Cones
2 East Lake Fissure
3 Deep Valley Fault
4 Sheeps Rump Cinder Cone
5 North Pumice Cone
6 North Obsidian Flow
7 Central Pumice Cone
8 Obsidian flow in vent of Central Pumice Cone
9 East Lake Obsidian Flows
10 Chain Craters on East Rim Fissure
11 Boundary: Lodgepole Pine to east/Ponderosa Pine to west
12 Little Crater Tuff Ring
13 Big Obsidian Flow
14 The Blowout
15 Plug Dome of Big Obsidian Flow
16 Rhyolite ridge
17 Sand Hill Cinder Cone

Letter and Pattern Symbols

B & dots	Basalt flows
P	Pumice flats
Stars	Cinder Cones (locations diagramatic along fissures 1 and 10)
Heavy lines	Faults and fissures
Solid	Obsidian flows

FIG. 4. Interpretation of classification of the Mt. Washington area.

Letter Symbols

CL	Clear Lake
BL	Big Lake
MW	Mt. Washington
SM	Scott Mountain
B	Area of Hoodoo Burn
S	Area of selective cutting of Ponderosa Pine forest
H126	Highway 126
M	Morainal ridges from Mt. Washington
W	Wind direction by ash dunes
E	Classification error
b	Brushy areas of interest
MS	Mostly cut block within area S

Pattern Symbols

Stars	Volcanic vents—all exactly located
Light dots	Older basalt lava flows
Heavy dots	Younger basalt lava flows
Solid	Lakes

Number Symbols

1 Nash Crater
2 Hoodoo Butte
3 Hayrick Butte
4 Sand Mountain Cones
5 Old Belknap flow with brush cover
6 Small burned area
7 Inaccessible Cone
8 Belknap Crater
9 Little Belknap Crater
10 South Belknap Crater
11 Anderson Creek flow with brush cover
12 Twin Craters
13 Hand Lake
14 Four-in-one Cone

TABLE 3. QUANTITATIVE COMPARISON OF SELECTED CLASSES.

Class	Area (acres)		Error
	Classified	Measured	%
Newberry Lithologic Classes			
Rhyolite obsidian flows	877	870	0.8
Bare basalt flows	721	588	24
Single basalt flow	77	128	−40
Single pumice flat	117	111	5
Water Classes			
Newberry lakes	2220	2600	−15
Big Lake (Mt. Washington)	196	185	0.06
Burn and Clearcut Classes			
Hoodoo Burn	5480	5180	6
Clearcuts (total of 6)	248	224	11

are not important in this area where basalt flows make up over 20 per cent of the total classification. While this age distinction is visible on color infrared reconstitutions of the area, a photo-interpreter cannot map the boundary as well as it is done here by computer.

WATER CLASSES

Water is present on both classifications and snow is present on the Mt. Washington classification. These are very prominent classes. Even very small lakes (for example, 13 on Figure 4) and snow patches are correctly classified. Quantitative comparisons are within one per cent (Table 3). The omission errors on the Newberry classification are largely accounted for by the basalt edge effect discussed ablve.

FOREST CLASSES

In general both stand density and tree species are significant in defining spectral signatures in the five forest classes. Thus the species names attached to the forest classes are not dependable beyond the original training set locations. In the Newberry area the distinction between the ponderosa pine and lodgepole pine classes holds along the west slope (11 on figure 3) but stand density probably controls much of the variation within the caldera. In the Mt. Washington area Forest-3 is a mixture of lodgepole pine and true fir stands. Forest-2 is a mixed class of douglas fir stands on the west (where the training set was selected) and ponderosa pine on the east. Forest-1 is a class that includes some of each of the other two. No quantitative evaluation of these classes is available. However, one significant classification error (E on Figure 4) is known to occur where a rather large area of forest is misclassified as brush. The first classes are based on very small spectral differences in the infrared bands (see Tables 1 and 2), which largely do not show on the photographic reconstructions. In addition to distinguishing different forest stands, these classes allow one to interpret details not otherwise possible. Thus, on the Newberry classification, Paulina Creek and other elements of the radial drainage of the volcano show through this class distinction. Most of the faults and fissures (Figure 3) are also distinguished in this manner. On the Mt. Washington classification the wind direction recorded by linear ash dunes is reflected in the forest class distinctions (W on Figure 4). No raining sets were taken in the northeastern corner of the Mt. Washington classification where selectively logged ponderosa pine is present. Some suggestion that a distinct class would have been possible is given by the combination of brush and Forest-2 that results from the classes used.

BURN AND CLEARCUT CLASSES

The Mt. Washington area has been clearcut on the west side and selectively logged on the northeast. Training sets selected from these clearcuts are separated into younger and older clearcuts on the basis of ground observations and air photo interpretation. The resulting classes are found to be accurate within about ten per cent, but the figure must be treated with caution because the areas of the individual clearcuts measured are small enough to approach the accuracy of the planimeter and probably involve considerable internal error. The age distinction is correctly maintained in the classification. The younger clearcuts are only a few years old and have little vegetation present. In 1967 a large forest fire created the Hoodoo Burn (B on Figure 4) in the northern part of the area.

The resulting class is within six per cent of the measured value (see Table 3).

Both burn and clearcut classes establish signatures for grass, brush, and other forms of low vegetation. Thus they classify more than the specific features of interest. From a thorough interpretation of these low vegetation classes many important features can be distinguished, (cf. Figure 4) such as areas of alpine vegetation on Belknap Crater, North Sister, and other peaks, numerous cinder cones and other volcanic vents, moraines from Mt. Washington, two areas of older lava flows, and selectively logged areas in the northeast corner of the classification. A small number of clearcut areas are classed as burn, suggesting that they may have been slash burned in about 1967. A small forest fire scar (6 on Figure 4) is classed as Clearcut-1, indicating that burns can be separated on the basis of age.

PHOTO INTERPRETERS PERSPECTIVE

Additional details, not readily apparent from the classes used, can be interpreted from the classifications (Figures 3 and 4). Some of these are readily apparent on the photographic imagery, but others are not. The computer program that we used fails as soon as geometric shape becomes important. Thus conical cinder cones and linear fractures cannot be classified although they are readily visible on the photographic imagery. The shading effects that make them visible on the imagery defeat the computer program. They can, however, be interpreted from the classifications. Figure 3 shows numerous faults and both cinder cones and some other volcanic vents. In general the cinder cones show up as a multiclassified area with one of the clear cut classes, the burn class, or the Newberry pumice class recording the bare area near the crest. On the Mt. Washington classification other special features that can be seen, but are difficult or impossible to see on the imagery, are U. S. Highway 126, morainal ridges west of Mt. Washington, and the orientation of linear ash dunes which record the wind direction at their time of deposition.

SPECTRAL RESPONSE

Details of spectral response will be considered only for the geologic materials as these are most unique to this investigation. The means and thresholds used for all 16 classes of the two areas are given on Tables 1 and 2. As our program does not yet collect statistics for the entire area classified, the data used are from the trainings sets selected for each class. As such, they represent the purest examples of each class available. Variations in spectral response and class separation for materials of geologic interest are shown on Figure 5. Of these, the two basalts (NB and WB) are very similar classes, being bare rock of an aa surfaced flow with only widely scattered shrubs

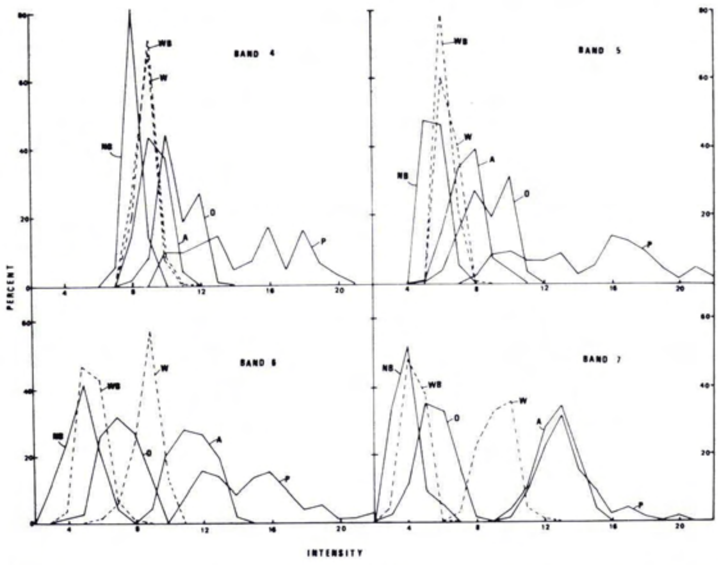

FIG. 5. Spectral responses and class separation for materials of geologic interest (P = pumice flats, O = obsidian, A = Newberry pumice, NB = Newberry basalt, WB = Mt. Washington younger basalt, and W = Mt. Washington older basalt).

as vegetation, and their spectral response is very similar. The older basalts (w) with scattered tree regrowth in the Mt. Washington area differ only in the two infrared bands. The rhyolite obsidian flows (O), which have extremely blocky surfaces, differ from the basalts largely by having slightly higher reflectances in all bands. The Newberry ash (A) and pumice flat (P) materials are quite similar substances with relatively high reflectances. Both are fragmental, vesicular rhyolitic material from explosive eruptions. The pumice flats are topographic flat areas covered with pumice and relatively little vegetation. Somewhat more forest is present in the ash areas and most of the surface is sloping. The reflectance spectra reproduced from the ERTS data are interesting to compare to laboratory data discussed by Rowan (1972). He shows that basalt has a decrease in reflectance in the near-infrared while rhyolite has an increase in the same range. This corresponds to the results for basalt and for pumice and ash, but differs from those for obsidian. Since the published spectra are for crushed samples, surface texture is probably important in the variation shown by the obsidian (Ross, et al., 1969).

Discussion and Conclusions

Classifications of two areas in central Oregon into 8 and 11 classes demonstrate the value of a user oriented and inexpensive program for utilizing ERTS-1 data. The classifications are evaluated both directly and from the perspective of a photo interpreter, and significant information is obtained in each manner. ERTS spectral signatures are established for the various lithologic classes. Costs of the classification system used here are low once the NASA data is reformated for the local system. Gray scales and training set selection for a large area such as the Mt. Washington classification cost about \$100 to \$150 in computer time, and the classifications themselves costs about \$20. Usually the classification is performed two or more times with different thresholds and classes so that the entire effort may cost less than \$200, or about \$0.002 per acre. Indirect costs such as ground truth acquisition, operator time, etc. are not available as this classification was not made with an overall intent to evaluate cost effectiveness.

Acknowledgments

The research discussed herein was partially supported by NASA Contract NAS 5-21831. Assistance in acquisition and evaluation of ground truth data by Glen Miller and Dave Mouat of the OSU Environmental Remote Sensing Applications Laboratory is gratefully acknowledged. Critical reading by Dave Paine and Ralph Shay significantly improved the manuscript.

References

Bauer, M. E., and Cipra, J. E., 1973, Identification of agriculatural crops by computer processing of ERTS MSS data: *Symp. on significant results obtained from ERTS-1*, NASA Sp-327, v. 1, p. 205-212.

Baumgardner, M. F., Kristof, S. J., and Henderson, J. A., 1973, Identification and mapping of soils, vegetation, and water resources of Lynn County, Texas, by computer analysis of ERTS MSS data: *Symp. on significant results obtained from ERTS-1*, NASA Sp-327, v. 1, p. 213-221.

Higgins, M. W., 1973, Petrology of Newberry Volcano, Central Oregon: *Geol. Soc. Am. Bull.*, v. 84, p. 455-488.

_________, 1969, *Air-fall ash and pumice lapilli deposits from Central Pumice Cove, Newberry Caldera, Oregon:* USGS Prof. Paper, 650-D, p. D26-D32.

Kirvida, L., and Johnson, G. R., 1973, Automatic interpretation of ERTS data for forest management: *Symp. on significant results obtained from ERTS-1*, NASA Sp-327, v. 2, p. 1075-1082.

Melhorn, W. N., and Sinnock, S., 1973, Recognition of surface lithologic and topographic patterns in southwest Colorado with ADP techniques: *Symp. on significant results obtained from ERTS-1*, NASA Sp-327, v. 1, p. 473-482.

Ross, H. P., Alder, J.E.M., and Hunt, G. R., 1969, A Statistical Analysis of the Reflectance of Igneous Rocks from 0.2 to 2.65 Microns: *Icarus*, v. 11, No. 1, p. 46-54.

Rowan, L. C., 1972, Near-infrared iron absorption bands: applications to geologic mapping and mineral exploration: *Fourth Annual Earth Resources Program Review (NASA)*, v. 3, p. 60-1 to 60-12.

Sattinger, I. J., and Dillman, R. D., 1973, Digital land use mapping in Oakland County, Michigan: *Symp. on significant results obtained from ERTS-1*, NASA Sp-327, v. 2, p. 1047-1054.

Taylor, E. M., 1968, Roadside geology Santiam and McKenzie Pass Highways, Oregon: *Oreg. Dept. Geol. and Min. Indust. Bull.*, 62, p. 3-34.

Thomson, F. J., and Roller, N. E. G., 1973, Terrain classification maps of Yellowstone National Park: *Symp. on significant results obtained from ERTS-1*, NASA Sp-327, v. 2, p. 1091-1096.

Vincent, R. K., 1973, Ratio maps of iron ore deposits, Atlantic City district, Wyoming: *Symp. on significant results obtained from ERTS-1*, NASA Sp-327, v. 1, p. 379-386.